AFCRL-63-203
JANUARY 1963

Instrumentation for Geophysics and Astrophysics
No. 24

Research Report

A Simplified Sonic Anemometer for Measuring The Vertical Component of Wind Velocity

J. CHANDRAN KAIMAL

METEOROLOGICAL RESEARCH LABORATORY PROJECT 7655

AIR FORCE CAMBRIDGE RESEARCH LABORATORIES, OFFICE OF AEROSPACE RESEARCH, UNITED STATES AIR FORCE, L. G. HANSCOM FIELD, MASS.

Requests for additional copies by Agencies of the Department of Defense, their contractors, and other government agencies should be directed to the:

Armed Services Technical Information Agency
Arlington Hall Station
Arlington 12, Virginia

Department of Defense contractors must be established for ASTIA services, or have their 'need-to-know' certified by the cognizant military agency of their project or contract.

All other persons and organizations should apply to the:

U. S. DEPARTMENT OF COMMERCE
OFFICE OF TECHNICAL SERVICES,
WASHINGTON 25, D. C.

AFCRL-63-203
JANUARY 1963

Instrumentation for Geophysics and Astrophysics
No. 24

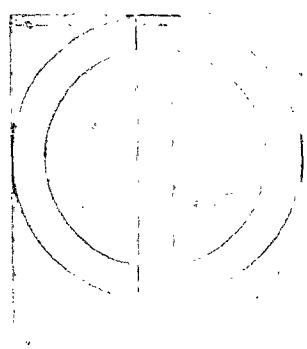

Research Report

A Simplified Sonic Anemometer for Measuring The Vertical Component of Wind Velocity

J. CHANDRAN KAIMAL

METEOROLOGICAL RESEARCH LABORATORY PROJECT 7655
AIR FORCE CAMBRIDGE RESEARCH LABORATORIES, OFFICE OF AEROSPACE RESEARCH, UNITED STATES AIR FORCE, L. G. HANSCOM FIELD, MASS.

Abstract

The design and operation of a continuous-wave sonic anemometer for measuring fluctuations in the vertical wind velocity component are described. Use of highly directional transducers has greatly simplified the design. Field tests show that the instrument responds to the vertical velocity fluctuations exactly as the more complicated but successful University of Washington sonic anemometer-thermometer. This system gives stable performance during prolonged continuous operation. The stability, accuracy, and simplicity make it a valuable tool for investigations of turbulence in the atmospheric boundary layer.

Contents

Illustrations

A Simplified Sonic Anemometer for Measuring the Vertical Component of Wind Velocity

1. INTRODUCTION

Successful application of the continuous-wave sonic technique for the measurement of the vertical velocity component has been demonstrated by Gurvich[1] and by Kaimal and Businger.[2] In both of these instruments two acoustic signals of different frequencies are transmitted in opposite directions along practically the same acoustic path, and the velocity component is determined from phase variations in the signals received at both ends of the path. Different frequencies are used so that effective use of band-pass and rejection filters can be made to reduce interference from cross-feed between the two channels. To extract the wind component from phase information contained in the two received signals, either of two methods has been utilized. Gurvich[3] uses heterodyning techniques to obtain two identical frequencies which are then compared directly for phase difference. Kaimal and Businger,[4] on the other hand, compare the phase of each received signal with that of a reference signal derived from the same source that drives the corresponding emitter; the wind information and also virtual temperature are then recovered by means of appropriate analog circuitry.

(Author's manuscript approved for publication, 18 December 1962)

The sonic anemometer described in this paper is the latest in a series of working attempts to develop the simplest possible sonic anemometer for measuring the vertical wind component. The simplification has been made possible through the use of highly directional transducers that, in turn, permit the use of identical frequencies in both channels. The circuitry is straightforward and compact and is designed so that, for normal operation of the instrument, no technical skill is required on the part of the operator.

2. BASIC THEORY

The sensing head is a four-transducer acoustic array similar to those described by Suomi,[5] Gurvich,[3] Stewart and Post,[6] and Kaimal and Businger.[4] Figure 1 shows the exact configuration of the transducers. E_1 and E_2 are the emitters for Channels 1 and 2, and R_1 and R_2 are the corresponding receivers. Assuming precise

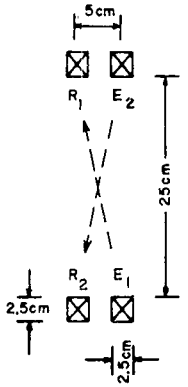

Figure 1. Transducer Configuration in the Acoustic Array

vertical orientation of the array, the phase difference $(\Delta\phi)_{1-2}$ between signals picked up at R_1 and R_2 (from emitters E_1 and E_2, respectively) can be expressed as

$$(\Delta\phi)_{1-2} = \frac{4\pi f d\, w}{C^2 - V^2} \qquad (1)$$

where f is the frequency of the signal applied to E_1 and E_2, d is the path length, C is the velocity of sound in still air, V is the total wind speed, and w is the vertical velocity component.† For wind speeds less than 35 m sec^{-1}, V^2 is at least

†Equation (1) is a simplification of the more general expression derived in Ref. 4.

two orders of magnitude smaller than C^2 and may be neglected. C^2 is not a quantity as directly measurable as d or f but may be expressed in either of two forms:

$$C^2 = \gamma R T^* \simeq \gamma R \overline{T}$$

or

$$C^2 = \frac{\gamma p}{\rho}$$

where γ is the ratio of the specific heats (c_p/c_v), R is the gas constant, T^* is the instantaneous virtual temperature, $\overline{T}$ is the mean air temperature used in computing the calibration factor for the sonic anemometer, p is the atmospheric pressure, and ρ is the density of air. The first relation is used if the velocity component as such is required. The second relation is particularly useful for eddy flux measurements. Thus Eq. (1) may be rewritten as

$$w = \frac{\gamma R \overline{T}}{4\pi f d}(\Delta\phi)_{1-2} \tag{2}$$

or

$$\rho w = \frac{\gamma p}{4\pi f d}(\Delta\phi)_{1-2} \ . \tag{3}$$

Equations (2) and (3) indicate that within the precision of the assumptions, $(\Delta\phi)_{1-2}$ is related linearly to w and ρw, respectively. Equation (2) is the less precise of the two expressions because of the assumption $T^* \simeq \overline{T}$ which is accurate only to within 1 percent, assuming no long-term trends in temperature. In Eq. (3), p is practically a constant since $\delta p/p$ is generally at least three orders of magnitude smaller than $\delta(\rho w)/(\rho w)$.

3. OPERATING CHARACTERISTICS

Figure 2 is a block diagram of the sonic anemometer. Barium titanate ultrasonic transducers (Type TR-7, Massa Industries, Division of Cohu Electronics) have been found to operate satisfactorily both as emitters and receivers. These have a resonant frequency of 40 kc and a narrow bandwidth of approximately 4 kc when connected in parallel (or series) with an 18-mh tuning choke. For the transducer configuration shown in Figure 1 the cross-feed signal is found to be at least

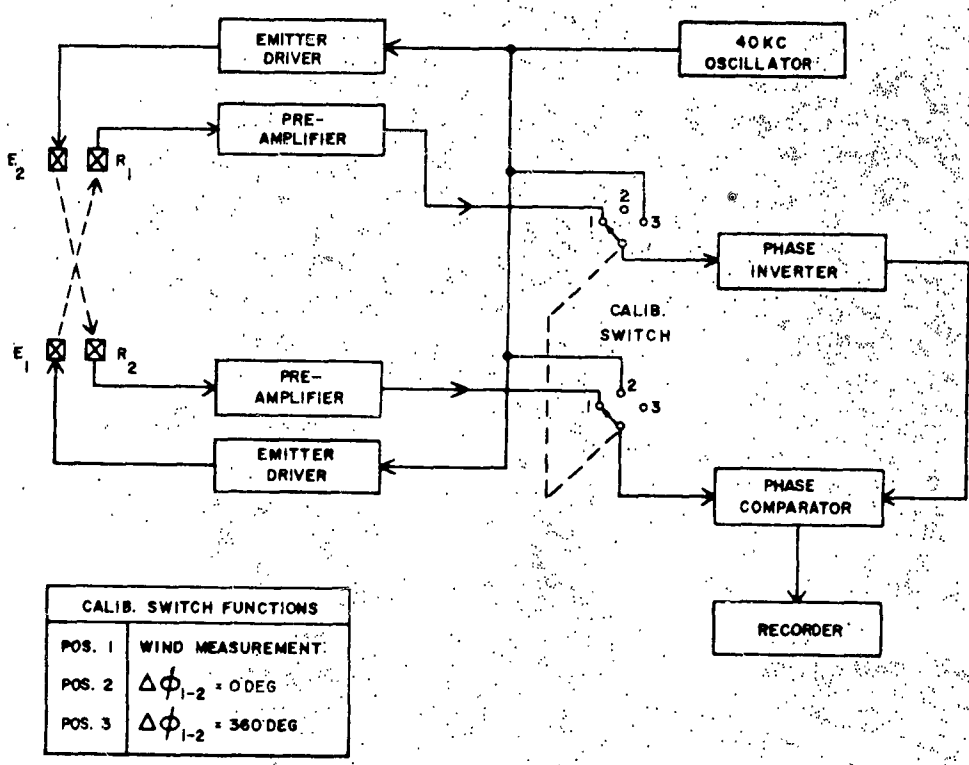

Figure 2. Block Diagram of the Sonic Anemometer

26 db below true signal level. The uncertainty introduced in wind measurement as a result of a cross-feed of this magnitude is small and can be neglected (see Section 4 for details). The acoustic array consisting of all four transducers, their supports, and boxes containing the preamplifiers and emitter-drivers is shown in Figure 3(a). One hundred feet of cable connects the acoustic array to the rest of the system, shown in Figure 3(b).

The preamplifier has three stages of amplification and a low impedance cathode-follower output as shown in Figure 4. Adequate rejection of background noise is achieved without recourse to electrical filters simply because of the highly selective response in the transducer. The emitter-driver (also shown in Figure 4) is simply a single-stage cathode follower. These circuits are located close to the transducers to avoid excessive transmission loss. Tuning chokes associated with the emitter and the receiver in each channel are adjusted for maximum signal level at the preamplifier output.

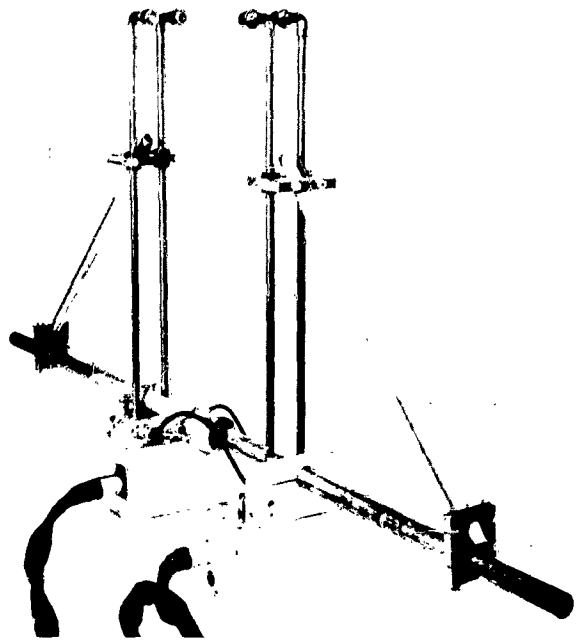

Figure 3(a). View of the Acoustic Array showing Construction Details. The array would be mounted in a vertical position for measuring w.

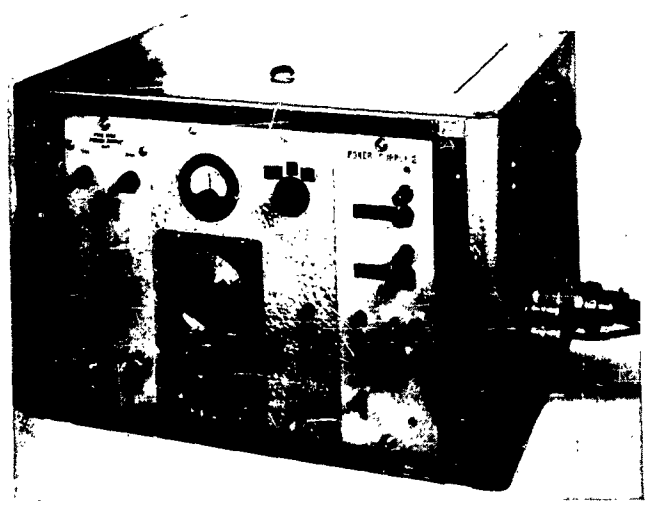

Figure 3(b). Front View of the Electronic Unit

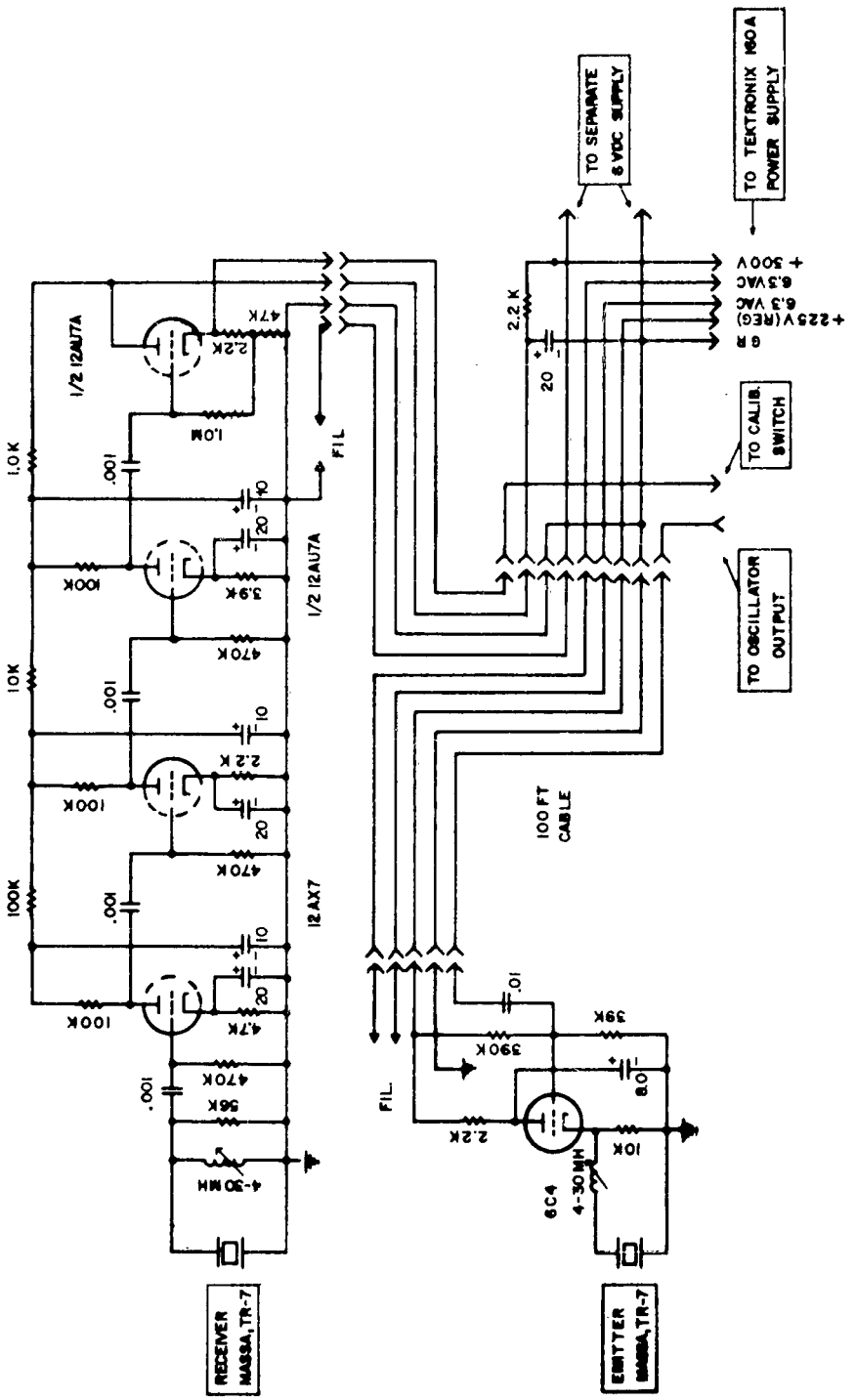

Figure 4. Schematic Circuit Diagram of the Preamplifier and Emitter-Driver

A variable frequency oscillator (Waveforms 510-B Module) with frequency setting at 40 kc and output at 1.0 volt is used as a signal source for driving the emitters and for calibrating the recorder.

Phase difference $(\Delta\phi)_{1-2}$ is obtained from direct phase comparison between output signals from preamplifiers in the two channels. The phase comparator circuit shown in Figure 5 is basically a 1 Mc bistable multivibrator triggered unsymmetrically by two sets of pulse trains obtained from the two signals to be compared. A pulse in each train corresponds to a zero-crossing in the positive direction of the original sinusoid. Wave shaping is achieved through successive operations involving limiting, differentiating, and clipping.

When the bistable multivibrator is triggered unsymmetrically in this manner, Section 1 (connected to Channel 1) stops conducting for a fraction of the period corresponding to $(\Delta\phi)_{1-2}$ and conducts for the remainder of the period, the total period being 25 μsec. This operation, when repeated, produces at the plate of that section a 40-kc rectangular wave, the duty cycle of which varies directly with $(\Delta\phi)_{1-2}$. In Section 2 (connected to Channel 2) the conducting and nonconducting periods are opposite to those in Section 1 and the waveform at that plate is consequently inverted. A center-zero microammeter connected as a voltmeter across the two plates will therefore indicate zero for 180° phase difference, full deflection to the left for 0°, and full deflection to the right for 360°. This meter (see Figure 5) provides a visual indication of the phase difference and is used primarily as a monitoring aid.

To obtain a voltage analog of the phase difference $(\Delta\phi)_{1-2}$ the waveform at the plate of Section 1 in the multivibrator is applied through a cathode follower to a zener diode stabilized clamping circuit, and finally to a simple low-pass filter. The clamping circuit ensures the constancy of the signal amplitude while the low-pass filter removes all the Fourier components in the rectangular wave and transmits merely the fluctuations associated with variations in the duty cycle.

The phase comparator described here can detect without ambiguity phase differences from 0° to 360°; but measurements very close to 0° and 360° are not possible because the multivibrator cannot distinguish between pulses in the two channels when they arrive almost simultaneously. A blind spot therefore occurs in the vicinity of 0° and 360°, and this is evident in Figure 6 which shows the response characteristics of the phase comparator. To avoid ambiguity in wind measurement it is necessary to confine operation of the comparator strictly within the linear range of operation. However, with transducer alignment as shown in Figure 1, the phase difference between the preamplifier output signals should ideally be 0° for zero vertical wind—a most unsatisfactory situation from the point of view of stability in the phase comparator. This can be avoided by introducing a phase inverter in one of the channels

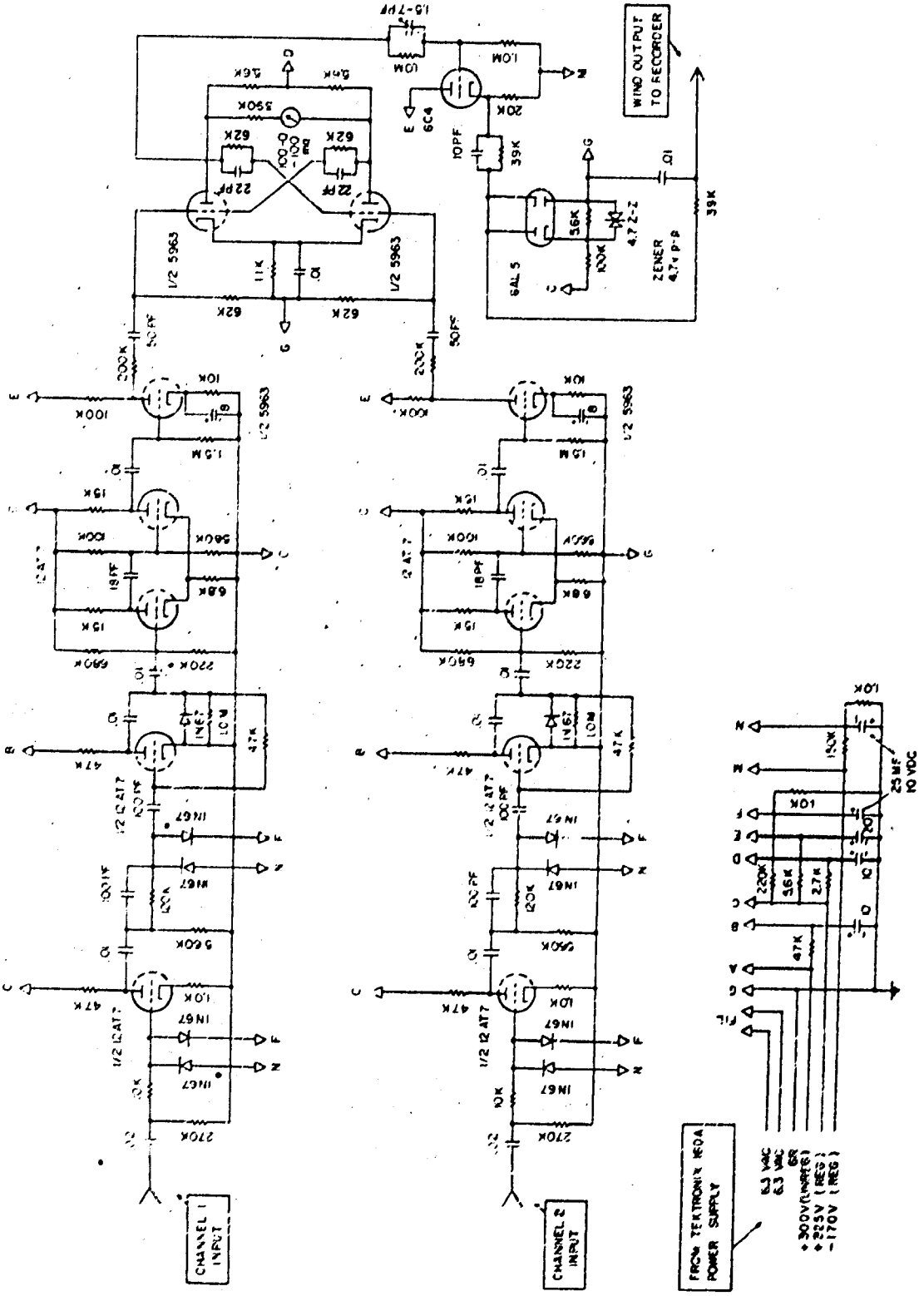

Figure 5. Schematic Circuit Diagram of the Phase Comparator

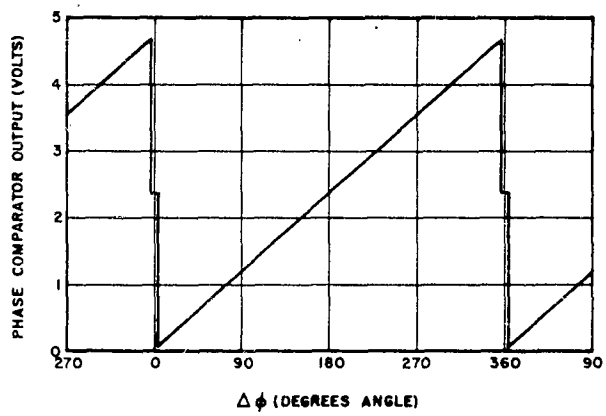

Figure 6. Response Characteristic of the Phase Comparator

as shown in Figure 2.† Now, 180° phase difference in the phase comparator corresponds to w = 0, and the limits 0° and 360° define the total range within which w can be measured without ambiguity. For f = 40 kc and d = 0.25 m this range corresponds to ±2.8 m sec^{-1} (for $\overline{T}$ = 280°K) on the w scale or ±0.335 gm cm^{-2} sec^{-1} on the ρw scale. This is an adequate range for w measurements.

To facilitate calibration of the recording device, a two-pole, three-position switch is provided, as shown in Figure 2. At Position 1 both receiver signals are applied to the phase comparator for normal wind measurement. At Positions 2 and 3 the preamplifier outputs are removed and the oscillator signal is applied directly to the phase comparator inputs, but to only one channel at a time. This causes continuous conduction in the half-section of the bistable multivibrator that has no signal input. Thus Position 2 of the calibration switch will produce an output reading corresponding to the true 0° (or full deflection to the left in the meter); and Position 3, an output reading corresponding to the true 360° (or full deflection to the right).

The calibration procedure is as follows. With the recorder in operation, the calibration switch is turned to Postion 2 for a few seconds and then to Position 3 for approximately the same interval. On the recorder, transition from Position 2 to 3 appears as a step change. The magnitude of this step change (which is precisely 360°) can be computed in terms of wind (or wind momentum) component. From this information a scale can be constructed for interpretation of the recorded fluctuations in meteorological units.

---

† Phase inversion can be achieved also by reversing the transducer leads in one channel. This, however, involves dismantling of the output connector in the TR-7 transducer. Both phase inversion techniques have been tried with equal success.

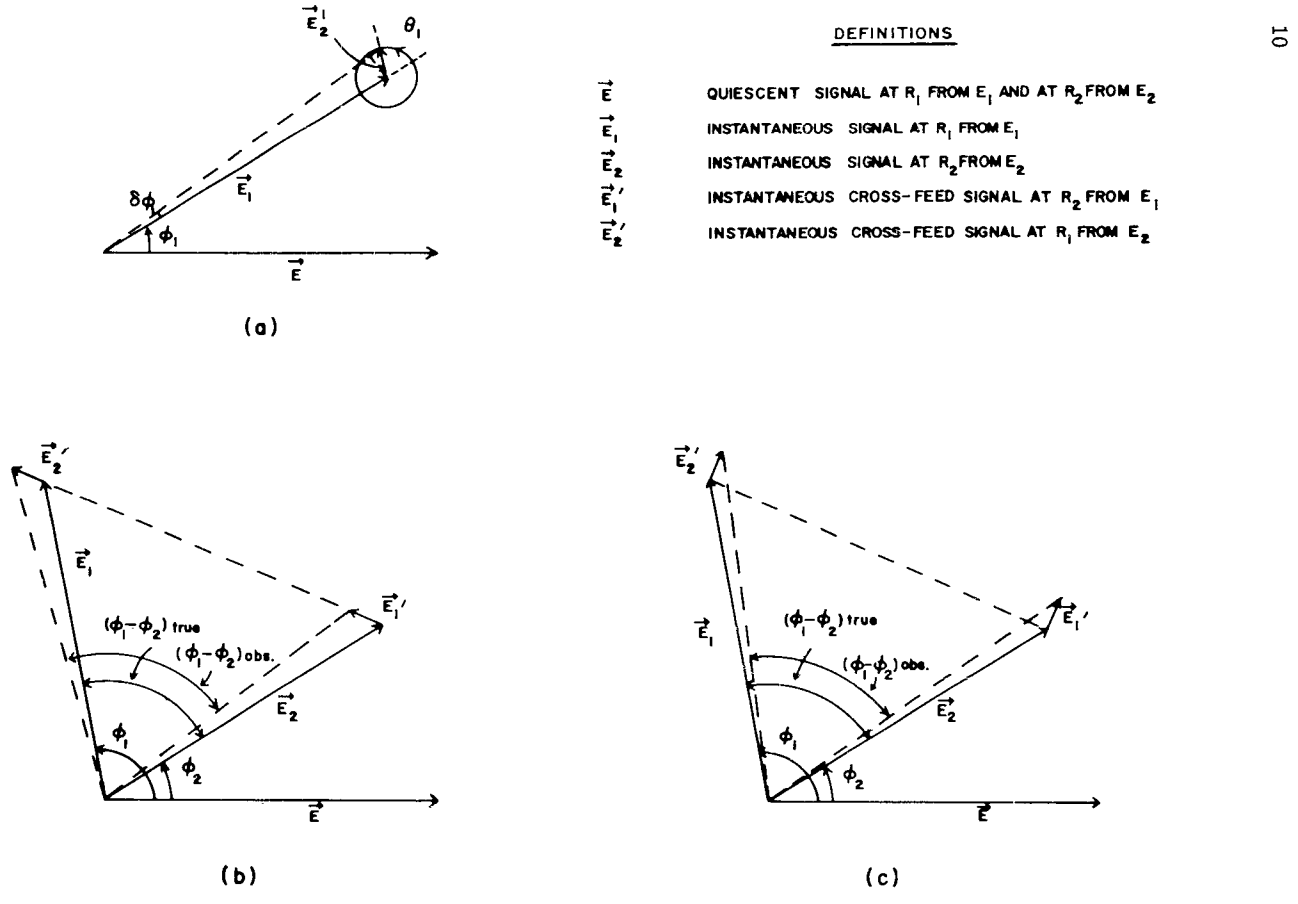

Figure 7. (a) Sound Vectors showing Error Introduced in Channel 1 as a Result of Cross-Feed from Channel 2; (b) Condition for Minimum Cross-Feed Error in the Phase Difference between Signals Received at R_1 and R_2; (c) Condition for Maximum Cross-Feed Error in the Phase Difference between Signal Received at R_1 and R_2

The analog nature of the instrument output makes it suitable for a variety of recording techniques. For preliminary tests, recordings have been made on a strip-chart recorder (Varian Model B-22). For actual field operation the data from several similar sonic anemometers will be recorded on a multichannel analog tape recorder and eventually digitized at an appropriate sampling rate for variance and spectral computations.

4. SYSTEM ACCURACY

Acoustic coupling between channels constitutes a major source of error in this system. At each receiver the true signal is found to be approximately 26 db higher than the level of the cross-feed signal. This corresponds to a voltage ratio of 20:1. The phase error introduced in Channel 1 as a result of interference from the cross-feed signal is represented vectorially in Figure 7(a). Following the same notations used in the figure, the phase error $\delta\phi_1$ may be expressed as a function of the magnitude and direction of the cross-feed signal $\vec{E}_2'$ with respect to the true signal $\vec{E}_1$. If θ_1 is the angle between $\vec{E}_1$ and $\vec{E}_2'$,

$$\delta\phi_1 \simeq \tan^{-1}\left[\frac{|\vec{E}_2'|}{|\vec{E}_1|}\sin\theta_1\right] \quad (4)$$

The angle θ_1 could be any value between 0° and 360°, but it is obvious that $\delta\phi_1$ is minimum when $\theta_1 = 0°$ or 180° and maximum when $\theta_1 = 90°$ or 270°. For a voltage ratio of 1:20 the maximum error amounts to approximately 2.85°.

The error $\delta\phi_2$ in Channel 2 may be expressed in a similar manner using notations consistent with Eq. (4):

$$\delta\phi_2 \simeq \tan^{-1}\left[\frac{|\vec{E}_1'|}{|\vec{E}_2|}\sin\theta_2\right] . \quad (5)$$

For wind measurements where only the phase difference $(\phi_1 - \phi_2)$ is of consequence, the error is not so large because of partial cancellation between $\delta\phi_1$ and $\delta\phi_2$. It is possible to compute the error in the observed $(\phi_1 - \phi_2)$ as a function of the true $(\phi_1 - \phi_2)$ on the basis of three assumptions: (1) that due to symmetry in the acoustic array $|\vec{E}_1| = |\vec{E}_2|$ and $|\vec{E}_1'| = |\vec{E}_2'|$; (2) that phase difference between $\vec{E}_1$ and $\vec{E}_2$ is zero for w = 0; and (3) that the phase difference between $\vec{E}_1'$ and $\vec{E}_2'$ is zero irrespective of the magnitude or direction of the horizontal wind component. No qualification is needed for the first two assumptions, but the third assumption is

true only if the transducer configuration is the same as in Figure 1, that is, with E_1 facing E_2 and R_1 facing R_2.

So long as these assumptions hold, the minimum error in the observed phase difference occurs when both the cross-feed vectors are parallel to the dashed line joining the end points of $\vec{E}_1$ and $\vec{E}_2$ in Figure 7(b). Ideally, for this condition, the phase errors in the two channels cancel each other. The maximum error in observed phase difference occurs when the cross-feed vectors are at right angles to the dashed line joining the end points of $\vec{E}_1$ and $\vec{E}_2$ in Figure 7(c). This maximum value may be expressed in a functional form as follows:

$$(\delta\phi_1 - \delta\phi_2)_{max} \simeq 2 \tan^{-1}\left[\frac{1}{20} \sin\left(\frac{\phi_1 - \phi_2}{2}\right)\right]. \qquad (6)$$

The plot of Eq. (6) shown in Figure 8 indicates that the actual uncertainty in the phase difference measurement is largest at the extreme ends of the scale and vanishes at zero phase difference. The accuracy is better than 5 percent throughout the entire scale down to the noise threshold (which, according to measurements, corresponds to approximately 0.5 cm sec^{-1}).

As a corollary to the above analysis it should be pointed out that if the circuitry is modified to measure $(\phi_1 + \phi_2)$ so as to obtain T^* fluctuations, such benefit from error cancellation as illustrated above will not be forthcoming.† A basic uncertainty of $\pm 5.7^\circ$ (amounting to approximately $\pm 0.15°C$) will exist in the temperature measurement.

Cross-feed between the two channels can also occur through mechanical coupling in the transducer supports. The use of separate pipe supports for each transducer has minimized this effect to the point where it is negligible compared to the cross-feed due to acoustic coupling.

Next in order of significance is the error due to misalignment in the acoustic array. The misalignment could be of a transient nature, arising from wind-induced vibrations in the transducer supports; or it could be of a permanent nature, such as from a bend in one of the supports. The first type introduces spurious fluctuations in the wind record, particularly if the supports are vibrating so as to cause a relative

†It is interesting to note that an expression analogous to Eq. (6) may be written for the temperature error which is maximum for the condition shown in Figure 7(b):

$$(\delta\phi_1 + \delta\phi_2)_{max} \simeq 2 \tan^{-1}\left[\frac{1}{20} \cos\left(\frac{\phi_1 - \phi_2}{2}\right)\right].$$

The plot of this function has the same shape as the curve in Figure 8 but is shifted 180° on the abscissa, implying that the temperature error is greatest for small values of w.

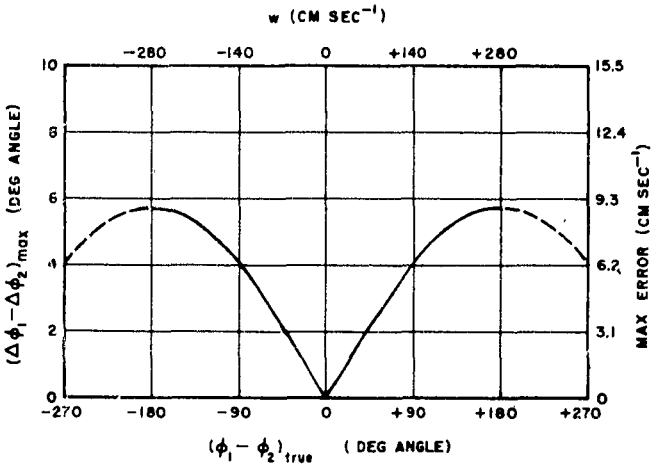

Figure 8. Maximum Cross-Feed Error Plotted as a Function of Phase Difference between Signals Received at R_1 and R_2

change in length between the two paths. A relative change in length of Δd will appear as a wind component of magnitude $\Delta d\, C/2d$. Specially designed braces are used in the acoustic array to keep this error low. The second type of misalignment will cause a shift in the position of zero wind on the record, thereby changing the absolute calibration; but it has relatively small effect on the wind scale itself. A simple calculation will clearly show that in order to maintain 1 percent accuracy in the absolute calibration the tolerance in head spacing is only 0.083 mm; whereas, for the same accuracy in the relative scale the tolerance is 2.5 mm. While in the present acoustic array the latter condition is easily fulfilled, the former cannot be approached even with careful handling of the array during transportation and installation. It is for this reason that no provision is made in the calibration scheme to determine the true zero position on the w scale.

Wake effects from the transducers constitute another potential source of error in sonic wind measurement; but this error is negligible so long as the acoustic path is normal to the mean flow, as is the case for w measurement. If the array is oriented for measuring horizontal velocity components, the heads will interfere with airflow along the acoustic path for winds blowing parallel to the path. Stewart and Post[6] have found that the turbulent wake created in front of the transducer pair on the upwind side of the array creates additional error by backscattering significant acoustic energy from the emitter into the receiver of the adjacent channel. This would appear as a random increase in the cross-feed signal at that receiver, much to the detriment of accuracy in the velocity component measurement. However their

experiments also show that the scatter component is negligible if the mean wind is normal to the acoustic path.

Another type of error could arise as a result of assumptions and approximations made in developing the theory. The only notable error in this case is the assumption that $T^* \simeq \overline{T}$ in Eq. (2). Short-term variations in T* would introduce an error of only 1 percent at the most in w. However long-term variations in T* can be significant since the scale calibration changes by approximately 1 percent for every $3^{\circ}C$ change in ambient temperature. To minimize this error a separate calibration should be made for each hour of observation, or more frequently if necessary. If the scale is calibrated in terms of ρw, the accuracy is unimpaired by changes in T* and, consequently, the calibration need be performed only once for any fixed setting of recorder gain.

The time constant of the electrical circuit is of the order of 1 msec (determined by the R-C combination at the output), but the spatial resolution of the instrument is obviously limited by the length of the acoustic path. The effect is to produce an artificial cutoff in the frequency spectrum for eddy diameters smaller than the acoustic path length. A crude estimate of the cutoff frequency f_c can be made by assuming that turbulent eddies are spherical in shape and are transported horizontally by the mean wind $\bar{u}$,

$$f_c = \frac{\bar{u}}{d} .$$

Theoretical discussion of errors helps in determining the reliability of any instrument, but nothing produces more confidence than direct proof of performance from comparison with another independent measurement. Figure 9 shows a sample from some of the comparison tests† made with the Kaimal and Businger instrument (University of Washington Sonic Anemometer-Thermometer) which has already been successfully tested in the field. The correlation is nearly perfect despite the fact that the two arrays were separated by a horizontal distance of approximately 1 meter and that the University of Washington Sonic Anemometer-Thermometer had a path length twice that of the AFCRL instrument. The slow response of the strip-chart recorder has probably smoothed out any differences in the high-frequency end of the w spectrum, but the evidence still points to the fact that the two instruments were indeed responding to the same atmospheric parameter with the same degree of accuracy.

---

†The comparison tests were conducted at the Round Hill Field Station as a joint effort by AFCRL, University of Washington, and Round Hill personnel.

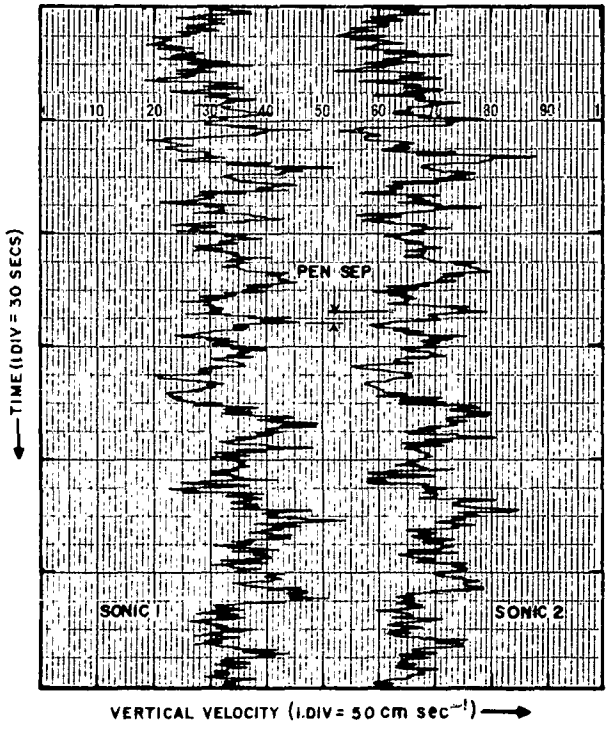

Figure 9. Simultaneous Recordings from the University of Washington Sonic Anemometer-Thermometer (Sonic 1) and the AFCRL Sonic Anemometer (Sonic 2). Scale indications refer to the main divisions shown by tick marks along the border.

5. CONCLUSIONS

Results from the comparison tests demonstrate that the sonic anemometer is operating satisfactorily. The simplification and reliability achieved as a result of using only one sonic frequency have indeed been worth-while; the error due to cross-feed is less than 5 percent of the measured velocity. The only loss incurred from this approach is the inability to make accurate temperature fluctuation measurements as well from a modification of the existing system.

From theory it is obvious that in any sonic anemometer the vertical component of wind velocity is measured with slightly less precision than the wind momentum

component. However this is an advantage as far as eddy flux measurements are concerned since $\overline{(\rho w)' x'}$ more accurately defines the eddy flux of the parameter x than the expression $\bar{\rho}(\overline{w'x'})$ generally used.

The transducer configuration is an optimum design for the particular transducers used. While this configuration is ideal for measuring w, it is not as well suited for measuring the horizontal wind components because of limited range and interference from transducer wakes.

Relative but not absolute calibration in the system can be maintained with better than 0.2 percent accuracy. For w' measurements this is not a serious disadvantage since, under conditions of steady state and horizontal homogeneity, $\overline{w}$ is zero.

The essential characteristics of the instrument are as follows:

Operating Range:	Approximately -2.8 to +2.8 m sec^{-1} in the w scale; approximately -0.335 to +0.335 gm cm^{-2} sec^{-1} in the ρw scale.
Accuracy:	Error less than 5 percent of observed reading in ρw; less than 6 percent in w.
Noise Level:	Less than 0.5 cm sec^{-1}.
Response Time:	Electrical response - approximately 1 msec.

Acknowledgments

The acoustic array, the preamplifiers, and 100-ft cable were designed and fabricated at Iowa State University of Science and Technology; the aluminum braces and mounting hardware were specially made for AFCRL at the University of Texas.

References

1. A.S. GURVICH, "Frequency Spectra and Functions of Distribution of Probabilities of Vertical Wind Velocity Components," Bull. (Izvestia) Acad. Sc. USSR Geophysical Series No. 7 (1960). (English Ed. Transl. by AGU, Jan 1961, pp. 695-703.)

2. J.C. KAIMAL and J.A. BUSINGER, "Preliminary Results from a Continuous Wave Sonic Anemometer-Thermometer," Jour. Appl. Meteor. (in press).

3. A.S. GURVICH, "Acoustic Micro-Anemometer for Investigating the Micro-Structure of Turbulence," Jour. Acoustics USSR (English transl. by Amer. Inst. Physics, Vol. 5, No. 3, pp. 375-376), (1959).

4. J.C. KAIMAL and J.A. BUSINGER, "A Continuous Wave Sonic Anemometer-Thermometer," Jour. Appl. Meteor. (in press).

5. V.E. SUOMI, "Energy Budget Studies at the Earth's Surface and Development of the Sonic Anemometer for Power Spectrum Analysis," AFCRC (Tech. Rep.) 56-274 Contract No. AF19(122)-461, Univ. of Wisconsin, Dept. of Meteorology (1956).

6. R.M. STEWART and R.E. POST, "The Sonic Anemometer," AFCRL (Final Rep.) 62-465 Contract No. AF(604)-2661, Iowa State Univ. of Science and Technology (1962).

AF Cambridge Research Laboratories, Bedford, Mass. Geophysics Research Directorate
A SIMPLIFIED SONIC ANEMOMETER FOR MEASURING THE VERTICAL COMPONENT OF WIND VELOCITY by J.C. Kaimal. December 1962.
17 pp. incl. illus. AFCRL-62-203
Unclassified report

The design and operation of a continuous-wave sonic anemometer for measuring fluctuations in the vertical wind velocity component are described. Use of highly directional transducers has greatly simplified the design. Field tests show that the instrument responds to the vertical velocity fluctuations exactly as the more complicated but successful University of Washington sonic anemometer-thermometer. This system gives stable performance during prolonged continuous operation. The stability, accuracy, and simplicity make it a valuable tool for investigations of turbulence in the atmospheric boundary layer.

UNCLASSIFIED

1. Anemometers
2. Sonic Anemometers
3. Meteorological Instruments

I. Kaimal, J.C.

UNCLASSIFIED

AF Cambridge Research Laboratories, Bedford, Mass. Geophysics Research Directorate
A SIMPLIFIED SONIC ANEMOMETER FOR MEASURING THE VERTICAL COMPONENT OF WIND VELOCITY by J.C. Kaimal. December 1962.
17 pp. incl. illus. AFCRL-62-203
Unclassified report

The design and operation of a continuous-wave sonic anemometer for measuring fluctuations in the vertical wind velocity component are described. Use of highly directional transducers has greatly simplified the design. Field tests show that the instrument responds to the vertical velocity fluctuations exactly as the more complicated but successful University of Washington sonic anemometer-thermometer. This system gives stable performance during prolonged continuous operation. The stability, accuracy, and simplicity make it a valuable tool for investigations of turbulence in the atmospheric boundary layer.

UNCLASSIFIED

1. Anemometers
2. Sonic Anemometers
3. Meteorological Instruments

I. Kaimal, J.C.

UNCLASSIFIED

AF Cambridge Research Laboratories, Bedford, Mass. Geophysics Research Directorate
A SIMPLIFIED SONIC ANEMOMETER FOR MEASURING THE VERTICAL COMPONENT OF WIND VELOCITY by J.C. Kaimal. December 1962.
17 pp. incl. illus. AFCRL-62-203
Unclassified report

The design and operation of a continuous-wave sonic anemometer for measuring fluctuations in the vertical wind velocity component are described. Use of highly directional transducers has greatly simplified the design. Field tests show that the instrument responds to the vertical velocity fluctuations exactly as the more complicated but successful University of Washington sonic anemometer-thermometer. This system gives stable performance during prolonged continuous operation. The stability, accuracy, and simplicity make it a valuable tool for investigations of turbulence in the atmospheric boundary layer.

UNCLASSIFIED

1. Anemometers
2. Sonic Anemometers
3. Meteorological Instruments

I. Kaimal, J.C.

UNCLASSIFIED

AF Cambridge Research Laboratories, Bedford, Mass. Geophysics Research Directorate
A SIMPLIFIED SONIC ANEMOMETER FOR MEASURING THE VERTICAL COMPONENT OF WIND VELOCITY by J.C. Kaimal. December 1962.
17 pp. incl. illus. AFCRL-62-203
Unclassified report

The design and operation of a continuous-wave sonic anemometer for measuring fluctuations in the vertical wind velocity component are described. Use of highly directional transducers has greatly simplified the design. Field tests show that the instrument responds to the vertical velocity fluctuations exactly as the more complicated but successful University of Washington sonic anemometer-thermometer. This system gives stable performance during prolonged continuous operation. The stability, accuracy, and simplicity make it a valuable tool for investigations of turbulence in the atmospheric boundary layer.

UNCLASSIFIED

1. Anemometers
2. Sonic Anemometers
3. Meteorological Instruments

I. Kaimal, J.C.

UNCLASSIFIED

AD

UNCLASSIFIED

UNCLASSIFIED

AD

UNCLASSIFIED

UNCLASSIFIED

AD

UNCLASSIFIED

UNCLASSIFIED

AD

UNCLASSIFIED

UNCLASSIFIED